Supporting Information for

Na^+/Vacancy Disordered Manganese-Based Oxide Cathode with Ultralow Strain Enabled by Tuning Charge Distribution

Siyuan Li,[a,#] Yangyang Zhang,[a,#] Kaixiang Lei,[a,*] Qian Yang,[a] Zheng Liu,[a] Kezhu Jiang,[a,*] Fujun Li,[b] Qiongqiong Lu,[c] Daria Mikhailova,[c] Shijian Zheng[a,*]

[a] State Key Laboratory of Reliability and Intelligence of Electrical Equipment, School of Materials Science and Engineering, Hebei University of Technology, Tianjin 300401, China

[b] Key Laboratory of Advanced Energy Materials Chemistry (Ministry of Education), College of Chemistry, Nankai University, Tianjin 300071, China

[c] Leibniz Institute for Solid State and Materials Research (IFW), Dresden e.V, Helmholtzstraße 20, D-01069, Dresden, Germany

[#]These authors contributed equally to this work.

*To whom correspondence should be addressed. E-mail: kaixianglei@hebut.edu.cn; sjzheng@hebut.edu.cn; fujunli@nankai.edu.cn

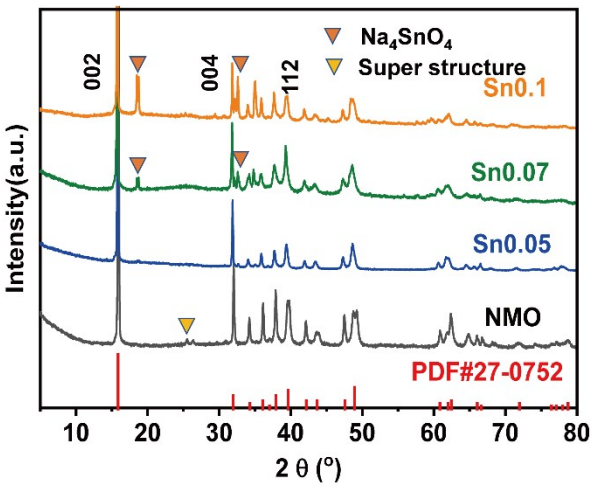

Fig. S1. XRD patterns of $Na_{0.67}Sn_xMn_{1-x}O_2$ (x=0, 0.05, 0.07, 0.10).

1 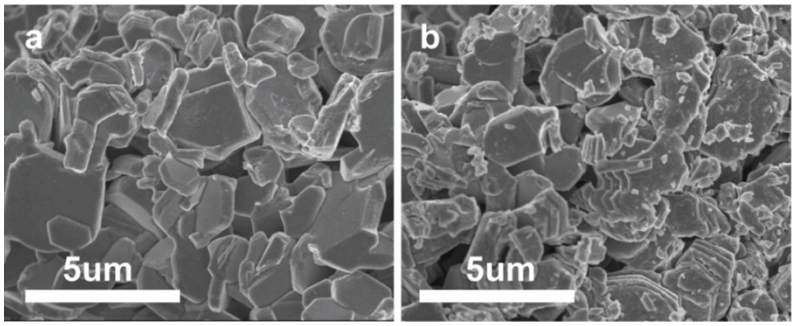

2 **Fig. S2.** SEM images of (a) NMO and (b) NSMO.

3

1 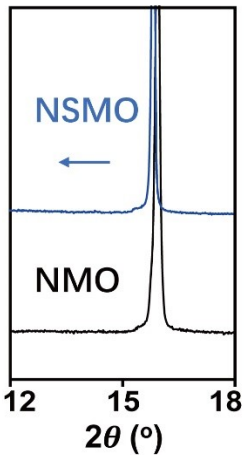

2 **Fig. S3.** Enlarged XRD patterns of NMO and NSMO from 12° to 18°.

3

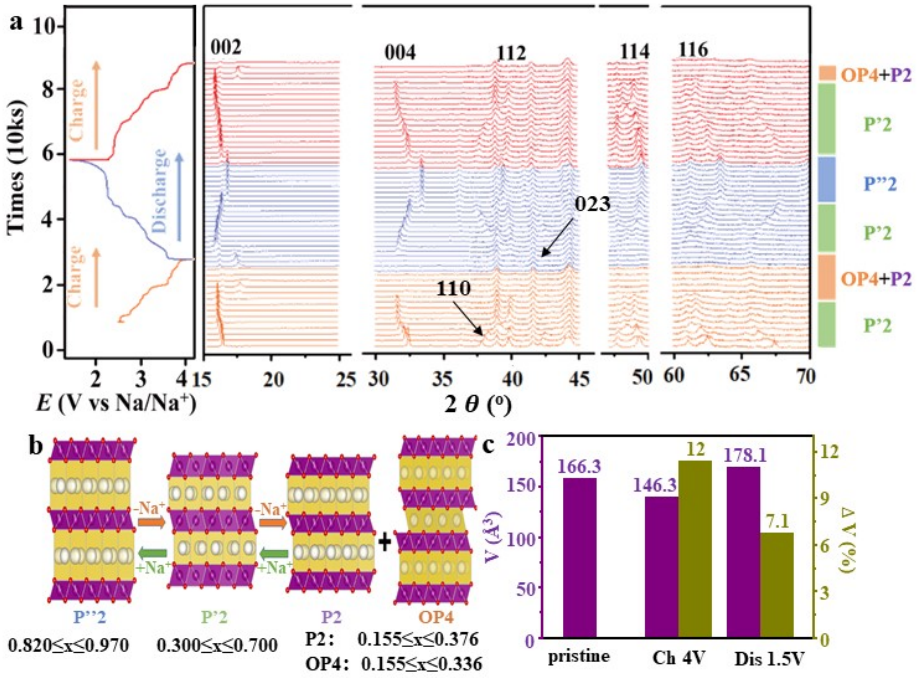

Fig. S4. Structural evolution of NMO electrode. (a) *In-situ* XRD patterns. (b) Illustration of phase transition during cycles. (c) Volume variations upon Na^+ extraction and insertion.

1 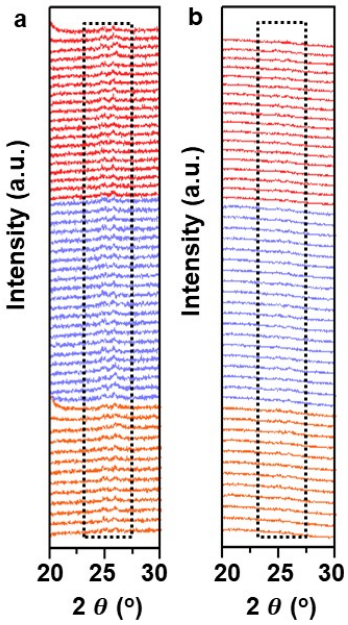

2 **Fig. S5.** Enlarged *in-situ* XRD patterns of (a) NMO and (b) NSMO between 20° and 30°.

3

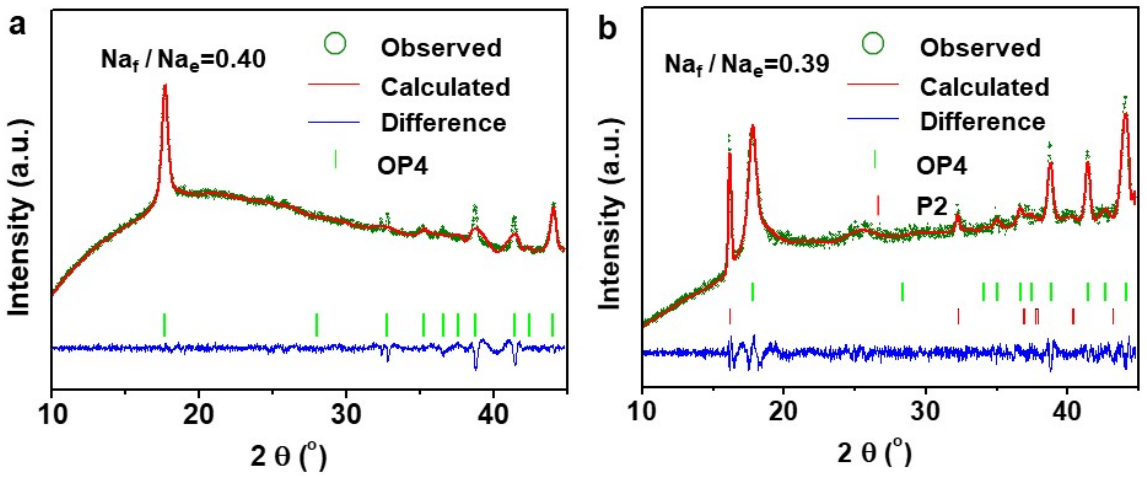

Fig. S6. Rietveld refinement profiles of the powder XRD data for the charged (a) NSMO and (b) NMO electrodes.

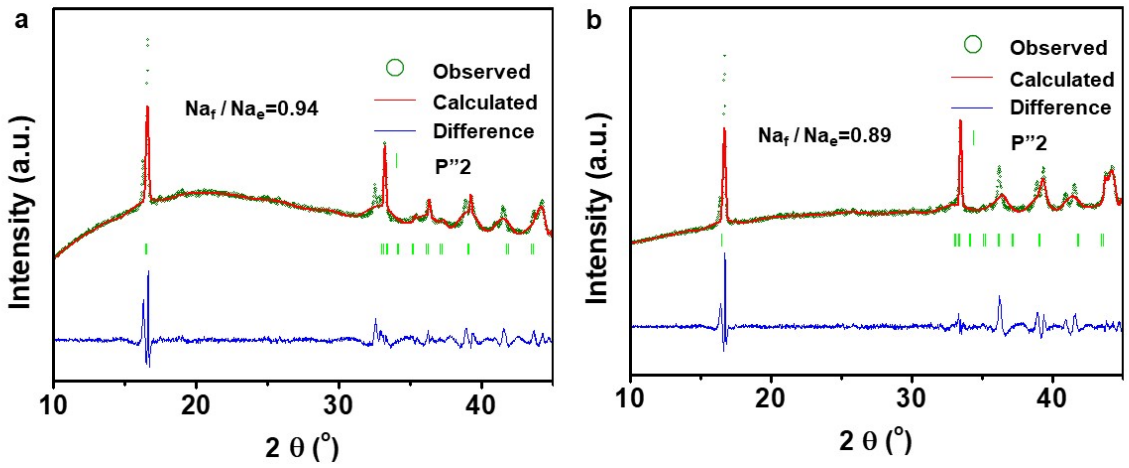

Fig. S7. Rietveld refinement of powder XRD data for (a) NSMO and (b) NMO electrodes cycled at 1.5 V.

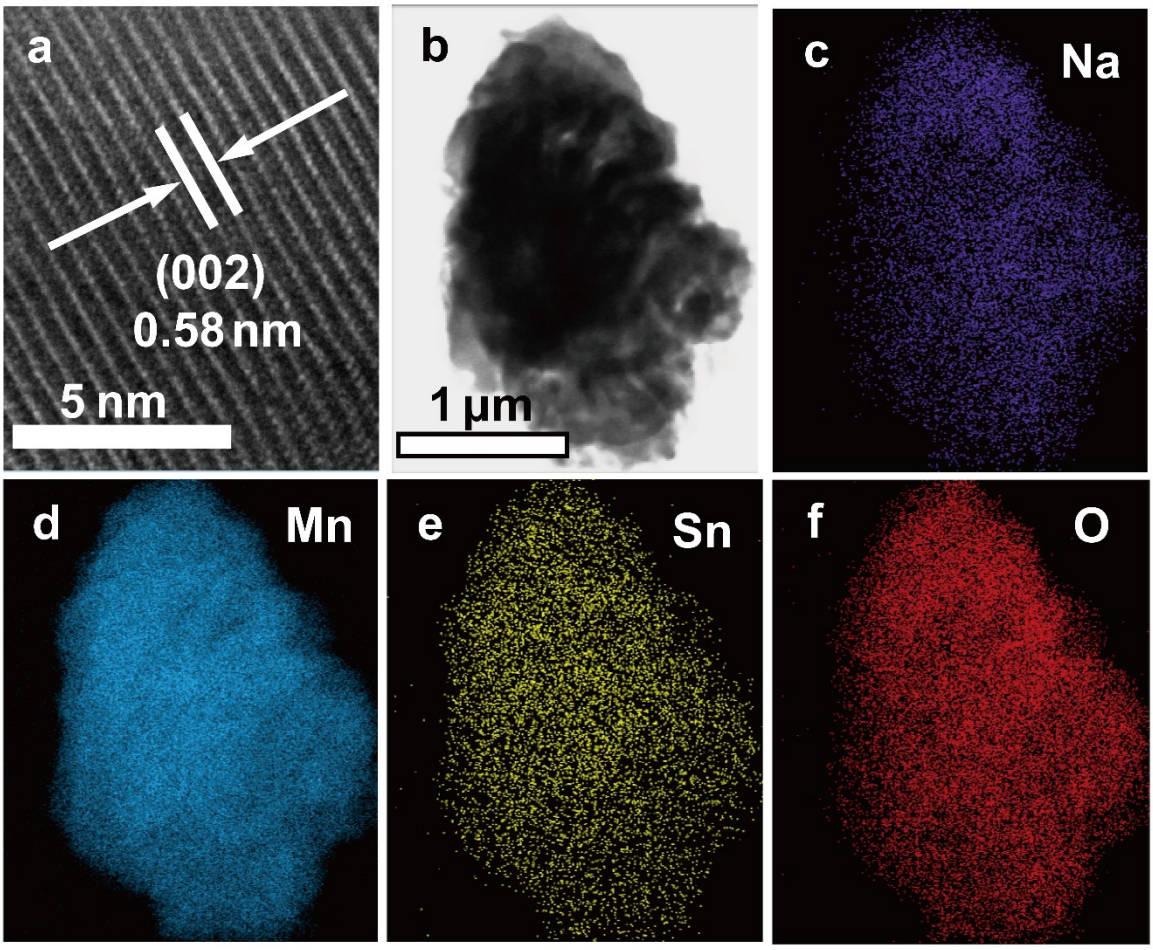

Fig. S8. (a) HRTEM image of NSMO after 10 cycles and (b-f) the corresponding EDS elemental mappings.

1 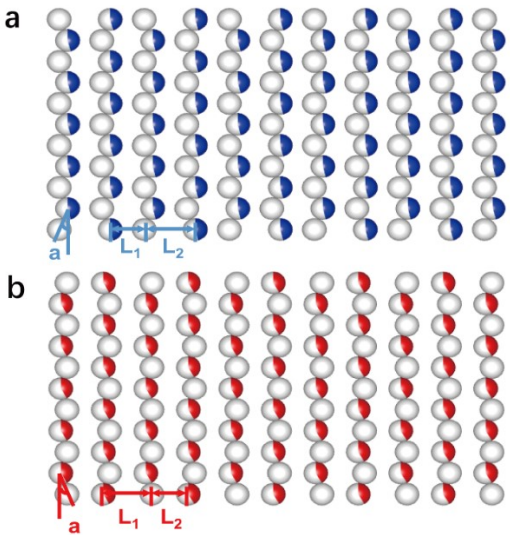

2 **Fig. S9.** Top view of the Na layers for (a) NMO and (b) NSMO based on XRD refined data.
3

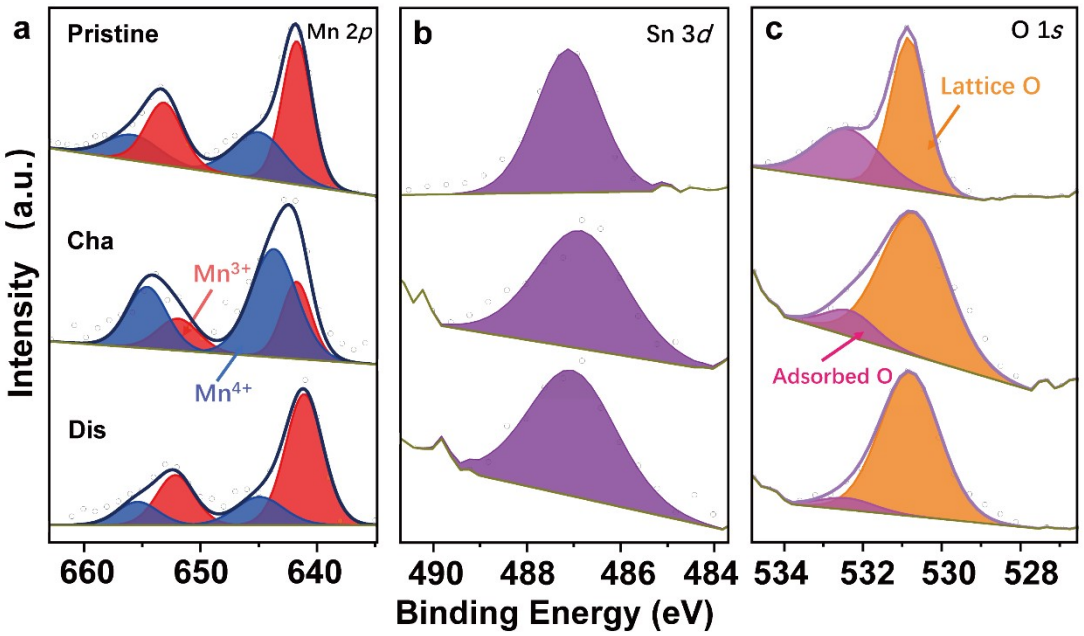

Fig. S10. Charge compensation mechanism of NSMO characterized by ex-situ XPS. (a) Mn 2p spectra. (b) Sn 3d spectra. (c) O 1s spectra.

1 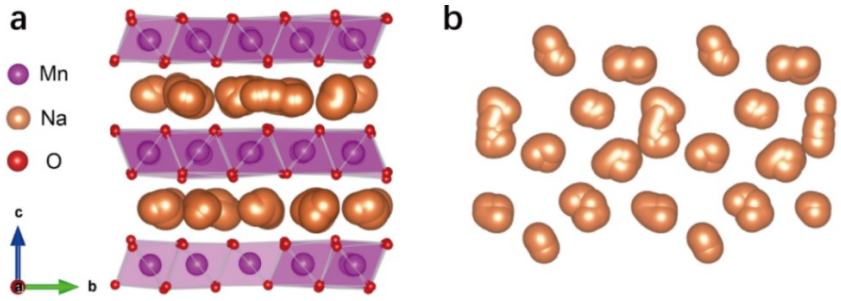

2 **Fig. S11.** (a) Trajectories of Na^+ in NMO simulated at 900 K. (b) Top view of Na layer.

3

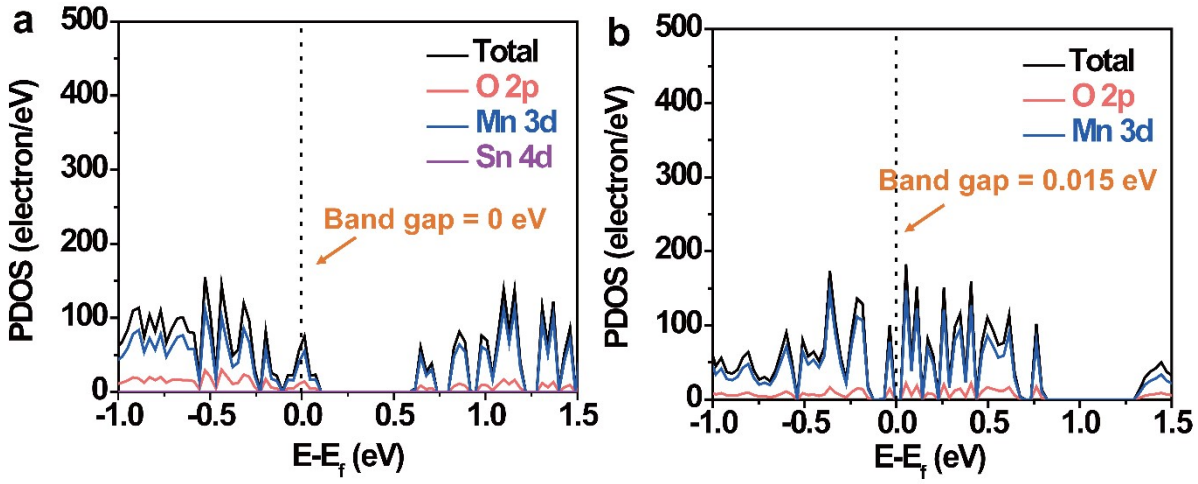

Fig. S12. The calculated DOS for NSMO (a) and NMO (b).

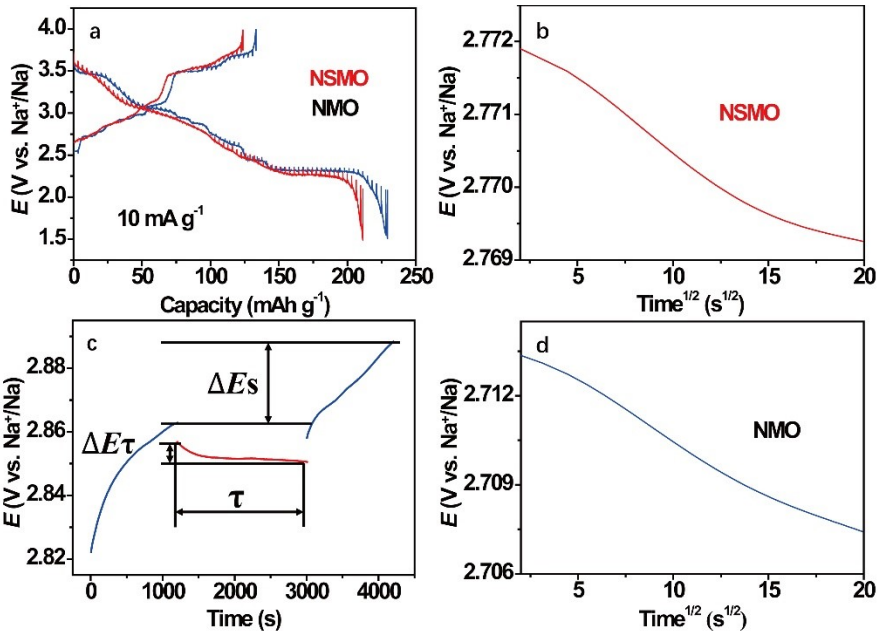

Fig. S13. (a) GITT curves of NMO and NSMO. The linear relationship between voltage (E) and square root of resting time ($Time^{1/2}$) for (b) NSMO and (d) NMO. (c) Current step diagram of the first desodiation of NMO at 2.535 V.

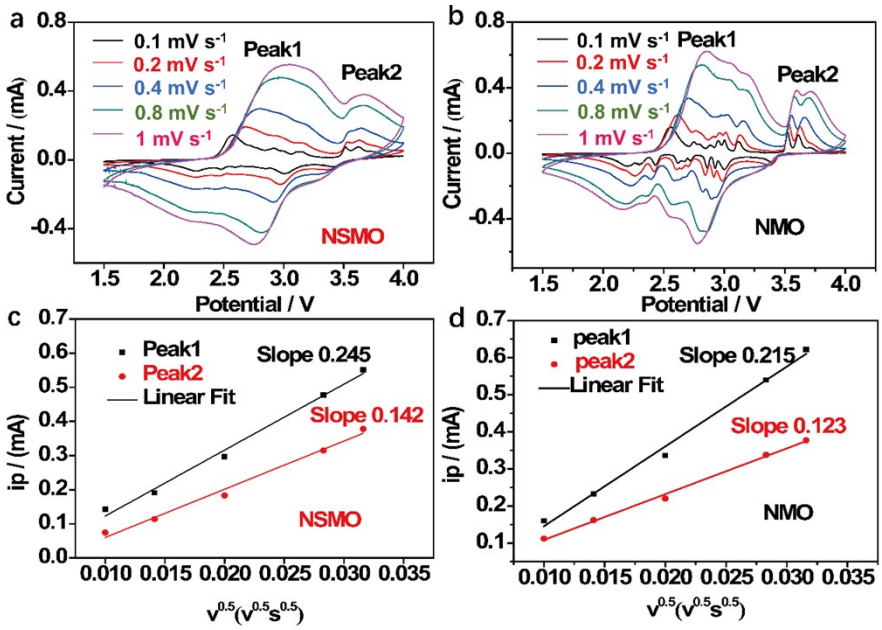

Fig. S14. CV curves of (a) NSMO and (b) NMO electrodes at different scan rates. Fitted plots of peak current (Ip) versus scan rate ($v^{0.5}$) square root for (c) NSMO and (d) NMO electrodes.

1 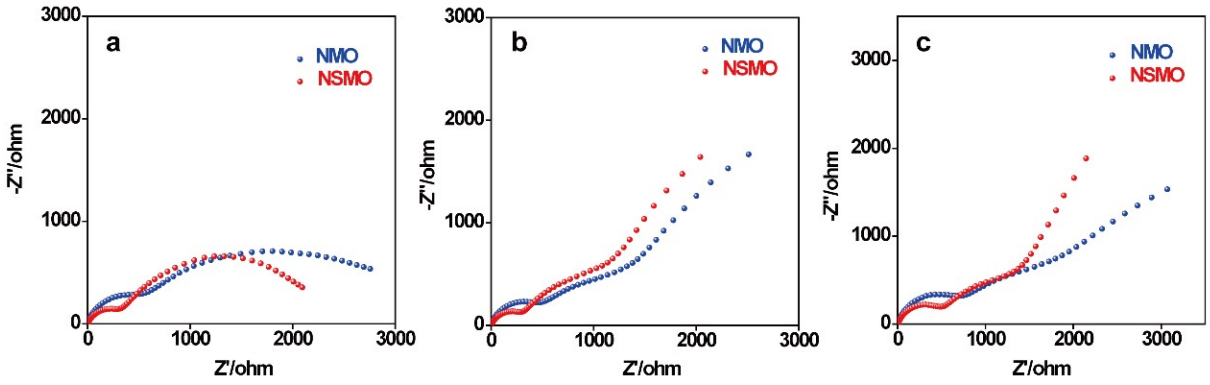

2 **Fig. S15.** EIS plots of NSMO and NMO (a) at open-circuit voltage and (b) after 1 cycle and (c) ten cycles.

3

1 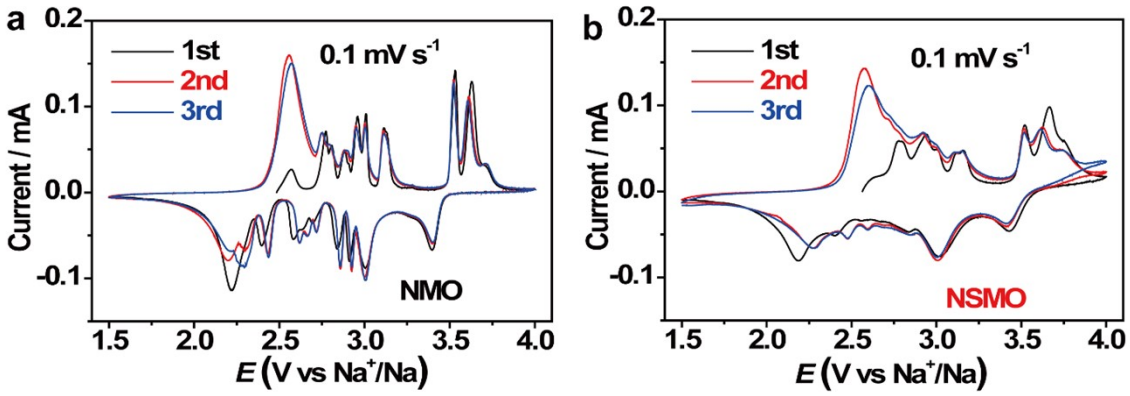

2 **Fig. S16.** CV curves of (a) NMO and (b) NSMO electrodes measured at 0.1 mV s^{-1} within 1.5-4.0 V.

3

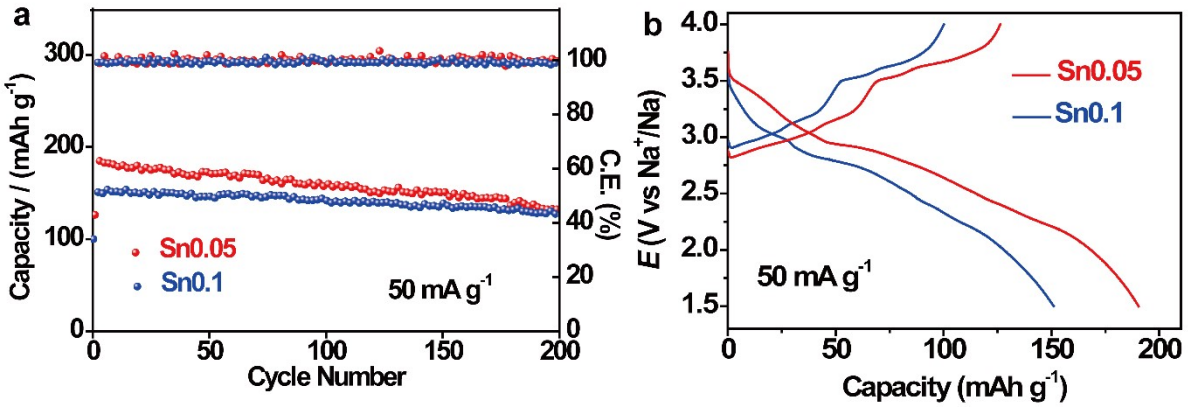

Fig. S17. (a) Cycle performance of NSMO and $Na_{0.67}Sn_{0.10}Mn_{0.90}O_2$ and (b) their selected charge/discharge curves.

1 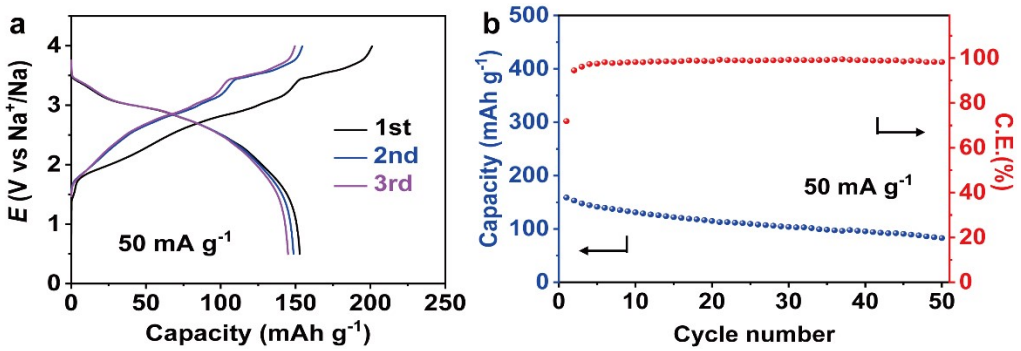

2 **Fig. S18.** (a) Charge/discharge profiles and (b) cycle performance of NSMO//HC full cells.

3

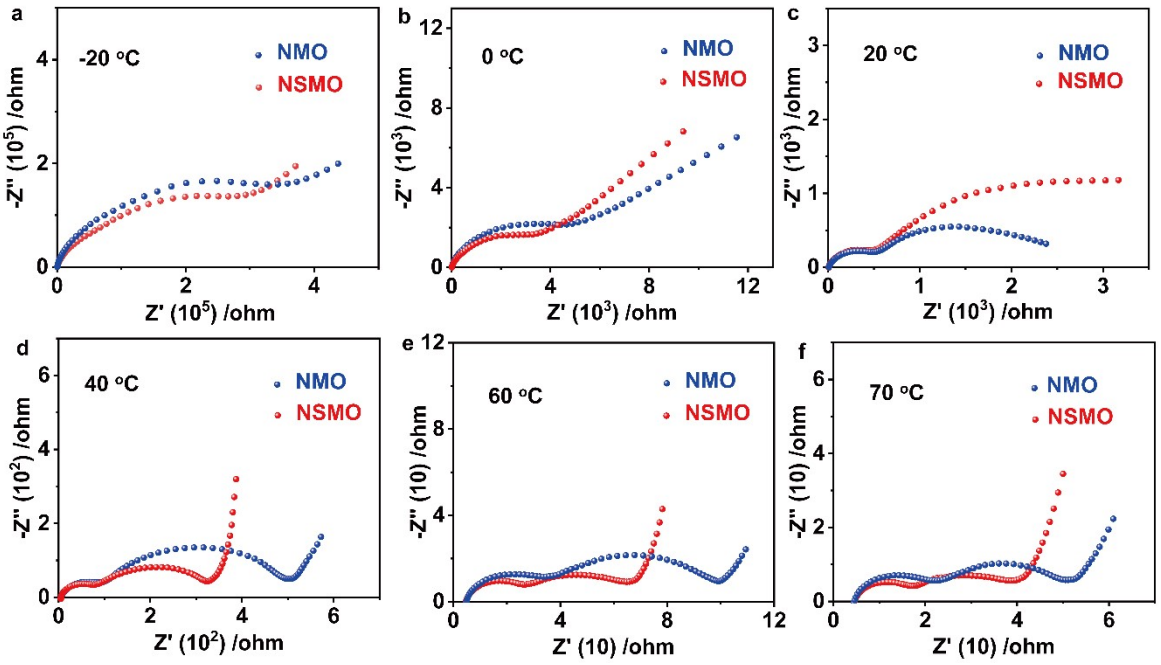

Fig. S19. EIS plots of NSMO and NMO at (a) -20 °C, (b) 0 °C, (c) 20 °C, (d) 40 °C, (e) 60 °C and (f) 70 °C under open-circuit voltage.

Table S1. Lattice parameters of NSMO based on Rietveld refinement.

Atom	Site	Occupancy	x	y	z
Na_f	4c	0.25(9)	0	0.113	0.250
Na_e	4c	0.41(1)	0	0.673	0.250
Mn	4a	0.95(5)	0	0	0
Sn	4a	0.45(5)	0	0	0
O	8f	1	0	0.675	0.890

Space group: *Cmcm,* a = 2.830 Å, b = 5.231 Å, c = 11.420 Å, α = β = γ = 90°, V = 169.059 $Å^3$, Rwp = 4.3%

Table S2. Lattice parameters of NMO based on Rietveld refinement.

Atom	Site	Occupancy	x	y	z
Na_f	4c	0.21(9)	0	0.236	0.250
Na_c	4c	0.45(1)	0	0.696	0.250
Mn	4a	1	0	0	0
O	8f	1	0	0.669	0.899

Space group: *Cmcm,* a = 2.831 Å, b = 5.240 Å, c = 11.209 Å, α = β = γ = 90°, V = 166.279 $Å^3$, Rwp = 4.3%

Table S3. Mn-O bond length, TMO_2 layer thicknesses, Na interlayer spacings, and distances between adjacent Mn columns for NSMO and NMO.

	$d_{(Mn-O)}$	$d_{(MnO2)}$	$d_{(O-Na-O)}$	$d_{(interslab)}$
NSMO (Å)	2.01/1.95	2.20	3.42	5.71
NMO (Å)	2.07/2.01	2.26	3.34	5.60
Change ratio	2.99%/3.08%	2.72%	2.34%	1.92%

Table S4. Refined structural parameters of OP4 phase in the charged NSMO electrode.

Atom	Site	Occupancy	x	y	z
Na_f	2d	0.04(1)	0.667	0.333	0.250
Na_e	2c	0.10(2)	0.333	0.667	0.250
Na1	2a	0.05(1)	0	0	0.5
Mn	4f	0.95	0.667	0.333	0.360
Sn	4f	0.05	0.667	0.333	0.360
O1	4f	0.5	0.333	0.667	0.415
O2	4e	0.5	0	0	0.296

Space group: *P63/mmc*, a = 2.952 Å, b = 2.952 Å, c = 22.188 Å, $\alpha = \beta = 90^o$, $\gamma = 120^o$, V = 167.449 $Å^3$, $\Delta V\% = 0.95\%$, Rwp = 1.9%

Table S5. Refined structural parameters of P''2 phase in the discharged NSMO and NMO electrodes.

Sample	Atom	Site	Occupancy	x	y	*z*
NSMO	**Na_f**	4c	0.45(2)	0	1.712	0.250
	Na_e	4c	0.47(6)	0	-4.154	0.250
	Mn	4a	0.94(3)	0	0	0
	Sn	4a	0.05(7)	0	0	0
	O	8f	1	0	1.473	-2.387
NMO	**Na_f**	4c	0.45(9)	0	0.645	0.250
	Na_e	4c	0.51(1)	0	0.646	0.250
	Mn	4a	1	0	0	0
	O	8f	1	0	0.199	-0.047

Space group: NSMO: *Cmcm*, a = 2.89 Å, b = 5.42 Å, c = 10.74 Å, α = β = γ= 90°, V = 168.23 Å^3, ΔV% = 0.49%, Rwp = 4.5%; **NMO:** *Cmcm*, a = 2.89 Å, b = 5.66 Å, c = 10.89 Å, α = β = γ = 90°, V = 178.13 Å^3, ΔV% = 7.1%, Rwp = 8%

Table S6. Refined structural parameters of OP4 and P2 phases in the charged NMO electrode.

Phase	Atom	Site	Occupancy	x	y	*z*
OP4	Na_f	2d	0.02(7)	0.667	0.333	0.250
	Na_e	2c	0.06(8)	0.333	0.667	0.250
	Na1	2a	0.03(5)	0	0	0.5
	Mn	4f	1	0.667	0.333	0.373
	O1	4f	0.5	0.333	0.667	0.402
	O2	4e	0.5	0	0	0.328
P2	Na_f	4f	0.00(5)	0.333	0.667	0.582
	Na_e	2b	0.00(5)	0	0	0.250
	Mn	2a	1	0	0	0
	O	4f	1	0.333	0.667	0.582

Space group: OP4: *P63/mmc*, a =2.99 Å, b = 2.99 Å, c = 18.87 Å, α = β = 90°, γ = 120°, V = 146.30 Å^3, ΔV% = 12%, Rwp = 3.6%, *wt*% = 83.8%; **P2:** *P63/mmc*, a = 2.82 Å, b = 2.82 Å, c = 11.24 Å, α = β = γ = 90°, V = 77.32 Å^3, ΔV% = 53.5%, Rwp = 3.6%, *wt*% = 16.2%

Table S7. Distances and angles between Na_f and Na_e in Na layers for P2-NMO, P'2-NMO and P'2-NSMO based on Rietveld refinement.

Sample	a (º)	L1 (Å)	L2 (Å)	ΔL (Å)
P2-NMO	60.0	1.6	3.3	1.7
P'2-NMO	20.5	2.1	3.2	1.1
P'2-NSMO	14.7	2.3	3.0	0.7

Table S8. Na^+ diffusion coefficients of peak 1 and 2 obtained by CV.

Peak	NSMO (cm^2s^{-1})	NMO (cm^2s^{-1})
1	2.25×10^{-10}	2.97×10^{-11}
2	2.26×10^{-11}	1.20×10^{-11}

Table S9. Electrochemical performance comparison of some reported cathodes in SIBs.

Materials	Cyclability (capacity retention)	Rate Capability	Ref
NSMO	131.2 mAh g^{-1} (71.63%) after 200 cycles at 50 mA g^{-1}	218.4 mAh g^{-1} at 10 mA g^{-1} 143.2 mAh g^{-1} at 500 mA g^{-1}	This work
poly(diphenylaminesulfonic acid sodium) (PDS)	72 mAh g^{-1} (70%) after 100 cycles at 50 mA g^{-1}	92 mAh g^{-1} at 100 mA g^{-1} 75 mAh g^{-1} at 200 mA g^{-1}	50
$NaFePO_4$	100 mAh g^{-1} (90%) after 240 cycles at 15.4 mA g^{-1}	120 mAh g^{-1} at 7.7 mA g^{-1} 46 mAh g^{-1} at 308 mA g^{-1}	51
$Na_{0.7}Mn_{0.6}Ni_{0.3}Co_{0.1}O_2$	69.6 mAh g^{-1} (58%) after 20 cycles at 9 mA g^{-1}	120 mAh g^{-1} at 9 mA g^{-1} 80 mAh g^{-1} at 185 mA g^{-1}	52
$Na_{0.66}(Mn_{0.54}Co_{0.13}Ni_{0.13})O_2$	60.5 mA g^{-1} (50%) after 100 cycles at 160 mA g^{-1}	121 mAh g^{-1} at 160 mA g^{-1} 94 mAh g^{-1} at 800 mA g^{-1}	53
$Na_{0.44}MnO_2$	75.0 mA g^{-1} (63%) after 60 cycles at 24.2 mA g^{-1}	102 mAh g^{-1} at 60 mA g^{-1} 98 mAh g^{-1} at 121 mA g^{-1}	54